



## Thioether-linked dihydropyrrol-2-one analogues as PqsR antagonists against antibiotic resistant *Pseudomonas aeruginosa*

Shekh Sabir<sup>a</sup>, Dittu Suresh<sup>a</sup>, Sujatha Subramoni<sup>b</sup>, Theerthankar Das<sup>c</sup>, Mohan Bhadbhade<sup>d</sup>, David StC. Black<sup>a</sup>, Scott A. Rice<sup>b</sup>, Naresh Kumar<sup>a,\*</sup>

<sup>a</sup> School of Chemistry, The University of New South Wales, NSW 2052 Sydney, Australia

<sup>b</sup> Singapore Centre for Environmental Life Sciences Engineering (SCELESE), Nanyang Technological University, 637551 Singapore, Singapore

<sup>c</sup> Department of Infectious Diseases and Immunology, School of Medical Sciences, The University of Sydney, NSW 2006 Sydney, Australia

<sup>d</sup> Mark Wainwright Analytical Centre, UNSW Sydney, Australia

### ARTICLE INFO

#### Keywords:

*Pseudomonas* quinolone system  
Quorum sensing inhibitors  
*Pseudomonas aeruginosa*  
PqsR antagonist  
Dihydropyrrol-2-one (DHP) analogues

### ABSTRACT

The *Pseudomonas* quinolone system (*pqs*) is one of the key quorum sensing systems in antibiotic-resistant *P. aeruginosa* and is responsible for the production of virulence factors and biofilm formation. Thus, synthetic small molecules that can target the PqsR (MvfR) receptor can be utilized as quorum sensing inhibitors to treat *P. aeruginosa* infections. In this study, we report the synthesis of novel thioether-linked dihydropyrrol-2-one (DHP) analogues as PqsR antagonists. Compound **7g** containing a 2-mercaptopyridyl linkage effectively inhibited the *pqs* system with an IC<sub>50</sub> of 32 μM in *P. aeruginosa* PAO1. Additionally, these inhibitors significantly reduced bacterial aggregation and biofilm formation without affecting planktonic growth. The molecular docking study suggest that these inhibitors bind with the ligand binding domain of the MvfR as a competitive antagonist.

### 1. Introduction

*Pseudomonas aeruginosa* is a highly opportunistic Gram-negative bacterium that is responsible for a number of nosocomial infections including pneumonia, cystic fibrosis, and urinary tract infection. These infections can be life-threatening especially in immunocompromised patients such as those battling cancer or HIV/AIDS.<sup>1,2</sup> *P. aeruginosa* is extremely resistant to several classes of antibiotics due to its highly evolved mechanisms of resistance, including efflux pump expression and biofilm formation.<sup>3</sup> In its recent report, the World Health Organization (WHO) listed *P. aeruginosa* as one of the critical priority pathogens which require urgent attention for the development of new therapeutics.<sup>4</sup>

*P. aeruginosa* secretes a wide range of virulence factors such as pyocyanin, rhamnolipids, exotoxins, elastases, which promote the invasion and damage of host tissue.<sup>5</sup> The ability to form biofilms is another important virulence characteristic of *P. aeruginosa*. A biofilm is typically an extracellular polymeric matrix made up of exopolysaccharides, nucleic acids, proteins, and lipids produced by bacterial cells. Significantly, bacterial cells in biofilm are 1000-fold more resistant to

antibiotics than isolated bacterial cells.<sup>6,7</sup>

To overcome bacterial resistance, the development of anti-virulence agents could be an effective alternative strategy.<sup>8,9</sup> Inhibitors that target virulence factors without killing bacterial cells should diminish the selective pressure on bacteria to develop drug resistance. In *P. aeruginosa*, virulence factor production and biofilm formation are primarily regulated by the quorum sensing (QS) system.<sup>10</sup> Therefore, QS inhibitors have the potential to reduce the severity of infections, allowing infections to be cleared by either the host immune system or by conventional antibiotic therapy.

QS is a bacterial cell density-dependent mechanism involving the production and release of several different chemical classes of small diffusible signalling molecules, known as autoinducers (AIs), which mediate intercellular communication.<sup>11</sup> As the bacterial cell number grows, the concentration of these AIs in the surrounding medium increases. Once the concentration of AIs reaches a certain threshold, the bacteria initiate collective behaviours including the production of virulence factors and biofilm formation.<sup>12</sup>

In *P. aeruginosa*, there are three major interconnected QS systems, namely the *las*, *rhl* and *pqs* systems. These QS systems are integrated and

\* Corresponding author.

E-mail addresses: [s.sabir@student.unsw.edu.au](mailto:s.sabir@student.unsw.edu.au) (S. Sabir), [subramoni@ntu.edu.sg](mailto:subramoni@ntu.edu.sg) (S. Subramoni), [das.ashishkumar@sydney.edu.au](mailto:das.ashishkumar@sydney.edu.au) (T. Das), [m.bhadbhade@unsw.edu.au](mailto:m.bhadbhade@unsw.edu.au) (M. Bhadbhade), [d.black@unsw.edu.au](mailto:d.black@unsw.edu.au) (D.StC. Black), [rscott@ntu.edu.sg](mailto:rscott@ntu.edu.sg) (S.A. Rice), [n.kumar@unsw.edu.au](mailto:n.kumar@unsw.edu.au) (N. Kumar).

<https://doi.org/10.1016/j.bmc.2020.115967>

Received 18 October 2020; Received in revised form 15 December 2020; Accepted 18 December 2020

Available online 1 January 2021

0968-0896/© 2020 Elsevier Ltd. All rights reserved.

control the activity of each other.<sup>13</sup> For example, the *las* system positively controls the *rhl* and *pqs* systems by activating the genes associated with their cognate receptors (rhlR and PqsR). The *las* and *rhl* QS systems utilize the *N*-acyl-*L*-homoserine lactone (AHL) class of signalling molecules for the activation of their cognate receptors lasR and rhlR respectively, while the *pqs* system utilizes alkyl quinolones, including 2-heptyl-4-hydroxyquinoline (HHQ) and 2-heptyl-3-hydroxy (4H) quinolone (PQS), to activate the receptor PqsR (MvfR) (Fig. 1).<sup>14,15</sup> Upon activation, PqsR upregulates the expression of several biosynthetic genes including the *pqsABCDE* operon, which further exerts positive feedback control of PQS biosynthesis and enhances virulence factor production as well as biofilm formation.<sup>16</sup> Synthetic PqsR receptor antagonists have been reported to reduce virulence factor production and biofilm formation in *P. aeruginosa*.<sup>17–20</sup> Additionally, a *P. aeruginosa* strain with mutant PqsR showed severely attenuated virulence factor production and biofilm formation in an animal infection model.<sup>21</sup> Therefore, targeting PqsR with synthetic small molecules could be a promising strategy to combat infections caused by antibiotic-resistant *P. aeruginosa*.

Dihydropyrrrol-2-one (DHP) and other structurally related compounds which mimic the natural *N*-acyl homoserine lactones (AHLs) have been reported by our group.<sup>22–24</sup> These compounds competitively inhibit the receptors of natural AHLs, leading to inhibition of QS and consequently the production of virulence factors and biofilm formation. Our group has also developed DHP analogues that showed QS inhibition against *P. aeruginosa* with minimal or no effect on bacterial growth.<sup>25,26</sup> Furthermore, attachment of DHPs to the surfaces of biomedical devices significantly reduced biofilm formation in *P. aeruginosa*.<sup>22–23</sup> DHPs have also been reported as competitive antagonists of the PqsR receptor, resulting in the inhibition of *pqs* signalling with micromolar potency.<sup>27</sup>

Additionally, small molecules containing substituted sulfur, thioether or disulfide functional groups have been reported as QS inhibitors, PqsR antagonists and/or biofilm inhibitors against *P. aeruginosa*.<sup>28–31</sup> In line with our continuous effort towards the development of DHP analogues as inhibitors of *P. aeruginosa* QS, we report herein the synthesis of novel thioether-containing DHP analogues by selective *Z*-bromination of the exocyclic double bond of the lactam, followed by a subsequent exchange reaction using different aromatic and aliphatic thiols. All the synthesized compounds were evaluated for the inhibition of *pqs* signalling, biofilm formation, pyocyanin production as well as tested for the effect on bacterial growth.

## 2. Results and discussion

### 2.1. Chemistry

The synthesis of DHP analogues involves condensation reaction of the commercially available phenyl acetone derivatives (1) with glyoxylic acid (2) in phosphoric acid, which gives an intermediate lactone compound (3). This lactone intermediate is subsequently converted into the corresponding lactam analogue (4) in sequential steps by using thionyl chloride followed by Aq-NH<sub>3</sub>. Finally, lactam compound dehydrated using phosphorous pentoxide which gives 5-methylene-4-phenyl-

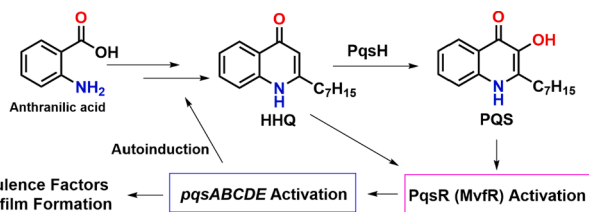


Fig. 1. Schematic diagram of the *Pseudomonas* quinolone quorum sensing (*pqs*) system, involving biosynthesis 2-heptyl-3-hydroxy (4H) quinolone (PQS) from anthranilic acid and activation of the PqsR (MvfR) receptor.

1,5-dihydro-2Hpyrrol-2-ones (5) (Scheme 1).<sup>24</sup>

To derivatize parent DHPs (5) containing an unsubstituted exocyclic double bond, we began by investigating monobromination reactions at the vinylic carbon. In initial attempts, treating compound (5) with 1 equiv. of *N*-bromo succinimide (NBS) in ACN gave the desired *Z*-brominated compound (6) in 55% isolated yield within 1 h at room temperature. Optimization experiments revealed that using 1,3-dibromo-5,5-dimethylhydantoin (DBDMH) with triethylamine in dichloromethane improved the yield, and Br-DHP compound (6) being isolated in up to 77% yield after 30 min at 0 °C (Scheme 2, Table 1).

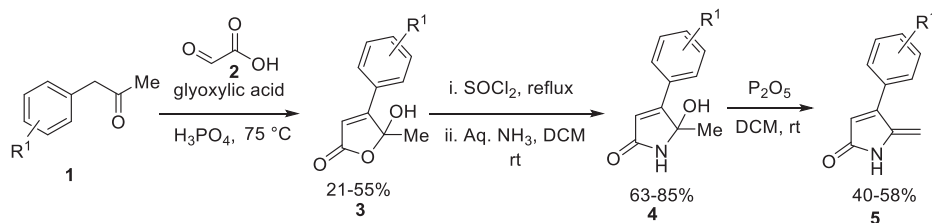
With the *Z*-brominated compounds (6) in hand, we were interested to investigate their exchange reactions with different nucleophiles as reported previously for bromo-thiolactone analogues.<sup>32</sup> However, our results suggested that bromo-DHPs were drastically less reactive than bromo-thiolactones, as no reaction was observed when the Br-DHPs (6) were reacted with aromatic or aliphatic amines at room temperature. On the other hand, the exchange reaction with thiophenol was successful and produced the thioether-linked DHP compound (7) in about 60% yield. Different aromatic thiols were then investigated and the use of 4-chlorothiophenol or 2-mercaptopyridine gave the desired thioether compounds in high yields under mild reaction condition (Scheme 2). However, the aliphatic thiol 1-propanethiol reacted very slowly and gave lower yields of product, as the starting Br-DHP was not fully consumed even after stirring for 2 days in the presence of excess thiol and base. The structures of all new DHP thioether compounds were characterised by <sup>1</sup>H and <sup>13</sup>C NMR spectroscopy and IR spectroscopy. Additionally, X-ray crystal analysis of compound (7c) was carried out to confirm the *Z* configuration of the final compounds (Supp. file).

### 2.2. *pqs* QS inhibition assay

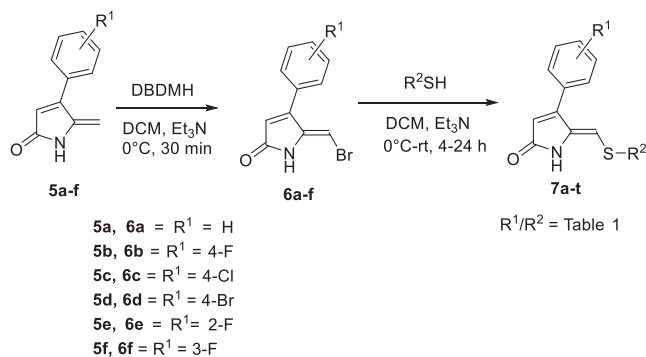
All the synthesized DHP thioether compounds were screened for PqsR inhibitory activity against the *P. aeruginosa* PAO1 *pqsA-gfp* reporter strain. This assay determines the expression of the *pqsABCDE* operon which is triggered by cognate receptor PqsR (MvfR). In the untreated control experiment the expression of the reporter reached its peak between 6 and 8 h and then decrease to its basal level. Most of the compounds inhibited the expression of the *pqs-gfp* reporter between 6 and 8 h in a dose-dependent manner. The thioether analogues (7a–7d) containing an unsubstituted phenyl ring at the C-4 position displayed moderate *pqs* inhibition ranges between 20% and 53% at 125 µg/mL concentration. A significant increase in *pqs* inhibition activity was observed with halogen-substituted (4-F phenyl) DHP analogue. The compound 7g bearing a 4-fluorophenyl ring at C4 and a 2-mercaptopyridyl group at the exocyclic position was the most potent *pqs* inhibitor overall, with 63% *pqs* inhibition at 125 µg/mL and a calculated IC<sub>50</sub> of 32 µM (Fig. 2, Table 2). However, the corresponding 4-Cl and 4-Br analogues 7k and 7o only showed weak inhibition of 18% and 20% respectively against *pqs* at 125 µg/mL. Compounds 7h and 7l having an *n*-propyl side chain displayed 59% and 62% inhibition against *pqs* activity respectively at 125 µg/mL, with calculated IC<sub>50</sub> values of 90 µM and 100 µM, respectively. Additionally, we found that the thiopyridine analogues 7s and 7t having fluoro at 2 and 3 position of phenyl ring are less active than the 4-fluoro analogue and displayed only 40% and 47% *pqs* inhibition, respectively.

### 2.3. Effect on bacterial aggregation and biofilm formation

We next investigated the effect of compounds 7g and 7l on bacterial aggregation and biofilm formation. The phase contrast microscopic images indicated that *P. aeruginosa* strains grown in presence of compounds 7g and 7l are hindered in their coaggregation ability. The impact of 7g and 7l in hindering *P. aeruginosa* ATCC and PAO1 aggregation in 24 h-old biofilm formation was clearly exhibited via microscopic images (Fig. 3). *P. aeruginosa* ATCC and PAO1 strains grown in presence of 7g and 7l showed less coaggregation (i.e. less decrease in its absorbance at



**Scheme 1.** General synthesis of dihydropyrrrol-2-one (DHP) analogues (5).



**Scheme 2.** Synthesis of dihydropyrrrol-2-one (DHP) thioether analogues.

**Table 1**  
Synthesized dihydropyrrrol-2-one (DHP) thioether analogues.

Compounds	R <sup>1</sup>	R <sup>2</sup>	Yields (%)
7a	H	<i>n</i> -Propyl	44
7b	H	Phenyl	60
7c	H	4-Cl-Phenyl	64
7d	H	2-Pyridyl	60
7e	4-F	Phenyl	92
7f	4-F	4-Cl-Phenyl	92
7g	4-F	2-Pyridyl	73
7h	4-Cl	<i>n</i> -Propyl	35
7i	4-Cl	Phenyl	80
7j	4-Cl	4-Cl-Phenyl	50
7k	4-Cl	2-Pyridyl	63
7l	4-Br	<i>n</i> -Propyl	37
7m	4-Br	Phenyl	78
7n	4-Br	4-Cl-Phenyl	70
7o	4-Br	2-Pyridyl	67
7p	2-F	<i>n</i> -Propyl	51
7q	2-F	Phenyl	87
7r	2-F	4-Cl-Phenyl	75
7s	2-F	2-Pyridyl	70
7t	3-F	2-Pyridyl	84

OD<sub>600nm</sub>) only about 11–13% and 13–18% respectively in two hours. Whereas its control exhibited significantly higher coaggregation rate about 23% for ATCC and 26% for PAO1. **7g** and **7l** showed radical decrease in *P. aeruginosa* aggregation in comparison to the control. Inhibition of *pqs* molecules in *P. aeruginosa* cell population plays a critical role in impeding biosynthesis of various essential molecules such as extracellular DNA (eDNA) which are responsible for coaggregation, colonization and biofilm formation. Most importantly earlier studies proved that *pqs* inhibition associated with debilitating phage mediated release of DNA in *P. aeruginosa* cultures and biofilms and eDNA encourages physio-chemical interactions that favours bacterial adhesion to the surface, coaggregation and scaffold for biofilm matrix.<sup>34–36</sup> Further, biomass quantification of 48 hr grown mature biofilm results suggest overall reduction of 20–25% in biofilm biomass in comparison to the control (Fig. 4). These results signify that these novel PqsR inhibitors would facilitate inhibition of pathogen colonization and biofilm formation.

## 2.4. Effect on bacterial growth

All the compounds were tested for their effect on the growth of bacteria at concentrations up to 125 µg/mL. None of the compounds inhibited the planktonic growth of bacteria up to the highest concentration tested (Fig. 5). This indicates that these DHP analogues inhibit *pqs* QS and biofilm formation of *P. aeruginosa* without interfering with bacterial growth, which should make them less likely to induce resistance.

## 3. Molecular docking study

To gain some understanding of the possible binding of 4-F phenyl DHP thiopyridyl analogue (**7g**) with the PqsR (MvfR) receptor, we performed an *in silico* molecular docking study using Discovery Studio software. Using the GOLD algorithm, energy minimized ligand **7g** was docked into the active site of a model created from the crystal structure of the MvfR protein (PDB: 6B8A) in complex with a previously reported competitive inhibitor **M-64** (IC<sub>50</sub> < 1 µM) (Fig. 6).<sup>37</sup>

The binding interactions of the highest-scoring pose (Gold score 52.27, pose 27) of **7g** present in the largest cluster (63%) were analysed. The phenyl moiety of compound **7g** showed π-alkyl hydrophobic interactions with Ala168, Leu197, Leu208, Val211, and Ile236. The nitrogen atom of the pyridine ring interacted via hydrogen bonding with Gln194, which was reported as one of the key amino acids for the competitive inhibition of PqsR.<sup>37</sup> Additionally, the carbonyl oxygen of the lactam interacts with Ser196 via a hydrogen bond (Fig. 7).

Besides the central ligand binding site of MvfR, there is an adjacent hydrophobic pocket lined by residues Leu183, Ile186, Leu189 and Tyr258 connected via a narrow channel to the main site. **M-64** occupies this additional hydrophobic pocket in MvfR<sup>LBD</sup> via hydrophobic interactions between its phenoxy group with the aforementioned amino acid residues. However, compound **7g** is unable to occupy this site due to its shorter side chain, which might be the reason for the lower PqsR antagonistic activity of **7g** compared to **M-64**.

## 4. Conclusion

In conclusion, a library of novel DHP thioether analogues has been synthesized and investigated for the inhibition of PqsR (MvfR) signaling and biofilm formation in *P. aeruginosa* PAO1. Most of the derivatives effectively blocked *pqs* QS with micromolar IC<sub>50</sub> values of these compounds. Dihydropyrrrol-2-one analogue bearing a 4-fluorophenyl ring and a 2-thiopyridyl linkage (**7g**) showed most potent activity with an IC<sub>50</sub> value of 32 µM. In addition, these analogues also disrupted bacterial aggregation and biofilm formation without affecting bacterial growth. The molecular docking study revealed that compound **7g** bound within the ligand-binding domain of PqsR, with similar interactions with a previously reported potent PqsR antagonist. Our future efforts will be focused on improving the potency of these inhibitors by lead optimization and structure–activity relationship analysis, including extension of the hydrophobic side chain to facilitate binding to the additional hydrophobic pocket of PqsR.

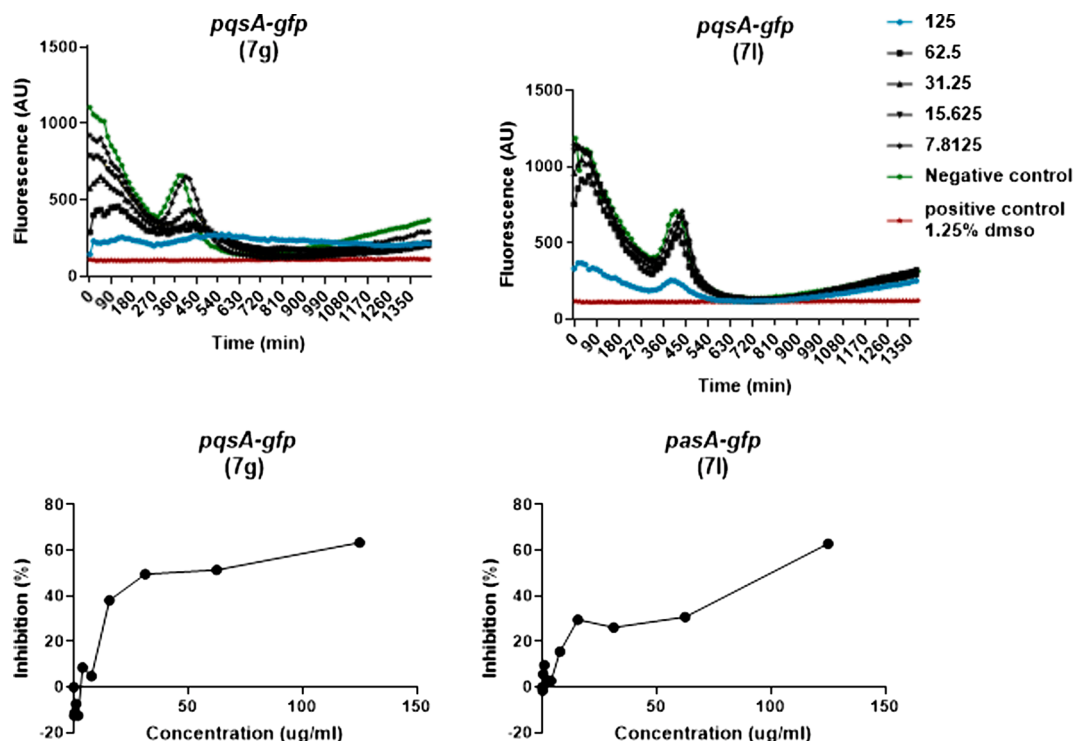


Fig. 2. Dose response curve and % Inhibition data of compound **7g** and **7i** in *pqsA-gfp* reporter assay in  $\mu\text{g/mL}$ . Negative control refers to 1.25% DMSO only and positive control refers to assay with a known inhibitor of *pqs*.<sup>33</sup>

Table 2

PqsR inhibition activity of the compounds using PAO1-*pqsA-gfp* reporter assay.

Entry	Compounds	(%) Inhibition (at 125 $\mu\text{g/mL}$ )
1	7a	20
2	7b	52
3	7c	43
4	7d	53
5	7e	45
6	7f	46
7	7g	63
8	7h	59
9	7i	45
10	7j	36
11	7k	18
12	7l	62
13	7m	52
14	7n	33
15	7o	20
16	7p	7
17	7q	42
18	7r	55
19	7s	40
20	7t	47

## 5. Experimental section

### 5.1. Synthesis

All the chemicals (reagents and solvents) were obtained from commercial sources (Chem-Impex Combi-Blocks, and Sigma-Aldrich) and used without further purification. Reactions were performed using oven-dried glassware under Argon atmosphere (if required). Room temperature (rt) refers to the ambient temperature. Reaction progress were monitored by thin layer chromatography (TLC) using precoated Merck silica gel 60 F254 plates and visualization using UV light (254 nm). Flash column chromatography was performed using Grace Davison LC60A 40–63  $\mu\text{m}$  silica gel as the stationary phase and solvent gradients of ethyl

acetate in hexane or methanol in dichloromethane used as mobile phase. Yields refer to the pure compounds isolated after flash column chromatography unless otherwise stated. Melting points of the new compounds were evaluated by using SRS MPA100 OptiMelt instrument and are reported without correction. IR spectra were recorded using Cary 630 ATR FTIR spectrophotometer. High-resolution mass spectrometry (HRMS) was performed by electrospray (ESI) ionization using a Thermo LTQ Orbitrap XL instrument at Bioanalytical Mass Spectrometry Facility (BMSF) of Mark Wainwright Analytical Centre (MWAC), UNSW Sydney.  $^1\text{H}$  and  $^{13}\text{C}$  NMR were recorded in deuterated solvents ( $\text{CDCl}_3$  and  $\text{DMSO-}d_6$ ) using Bruker Avance III 300 and Bruker Avance III 400 MHz instruments (Bruker Pty Ltd, Preston, Australia) at 24 °C. Chemical shifts ( $\delta$ ) are reported as relative to the corresponding solvent peak, with tetramethylsilane as the internal standard and quoted in parts per million (ppm). The coupling constants ( $J$ ) are reported in hertz (Hz). X-ray crystallography was carried out using single crystal XRD analysis and data have been deposited in the Cambridge Crystallographic Data Centre: Compound **7c**- Deposition Number 2027653.

**General procedure (A) for bromination of DHP:** DBDMH (1.8 mmol) was added in portions to a solution of DHP **1** (3.0 mmol) and  $\text{Et}_3\text{N}$  (3.0 mmol) in dry DCM (25 mL) at 0 °C. The reaction was stirred at 0 °C for 30 min, and the reaction progress was monitored by TLC. After complete conversion, a saturated solution of  $\text{NH}_4\text{Cl}$  (10 mL) was added. The mixture was extracted with DCM ( $3 \times 10$  mL), the extract dried with anhydrous  $\text{Na}_2\text{SO}_4$  and concentrated. The crude product was purified with silica gel flash column chromatography eluting with 30–40%  $\text{EtOAc}:\text{Hex}$ , and the desired compound (**6**) was isolated as a white/off-white solid in 60–77% yield.

(*Z*)-5-(bromomethylene)-4-phenyl-1,5-dihydro-2H-pyrrol-2-one (**6a**): Following the general procedure A, the title product was obtained as an off-white solid (451 mg, 60% yield); mp 118–120 °C;  $^1\text{H}$  NMR (300 MHz,  $\text{CDCl}_3$ )  $\delta$  8.00 (s, 1H), 7.50–7.44 (m, 3H), 7.40 (m, 2H), 6.28 (d,  $J = 1.8$  Hz, 1H), 6.11 (s, 1H).  $^{13}\text{C}$  NMR (76 MHz,  $\text{CDCl}_3$ )  $\delta$  169.94, 150.52, 141.66, 131.10, 130.07, 129.31, 129.13, 128.88, 128.58, 128.47, 122.02, 92.86; IR (ATR):  $\nu_{\text{max}}$  3154, 3109, 3029, 2762, 1886, 1687,

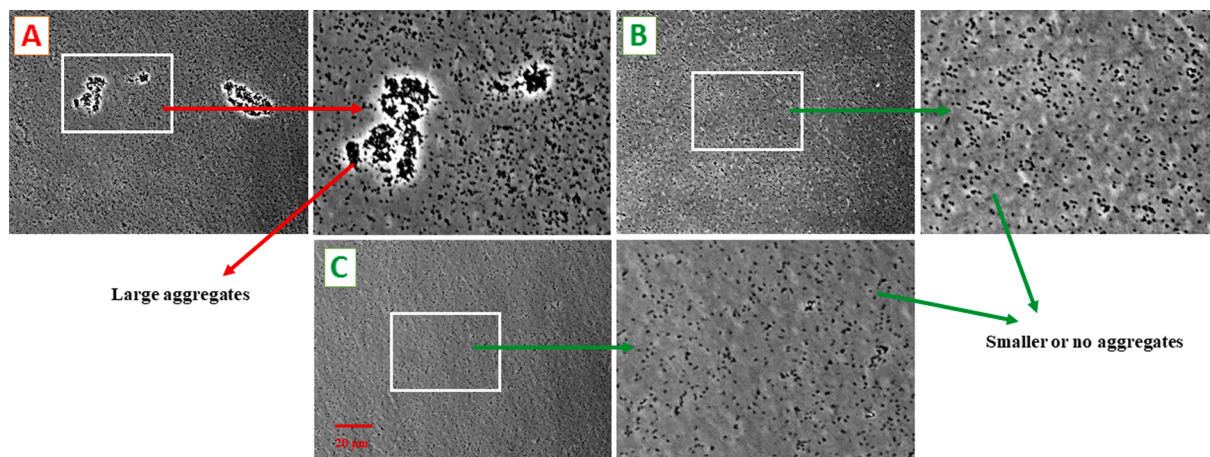


Fig. 3. Phase-contrast microscopy images showing aggregation of *P. aeruginosa* PAO1 grown in the presence of (A) Dimethyl sulfoxide (DMSO) only; (B) 250  $\mu\text{M}$  7g (C) 250  $\mu\text{M}$  71. Scale bar = 20  $\mu\text{m}$ .

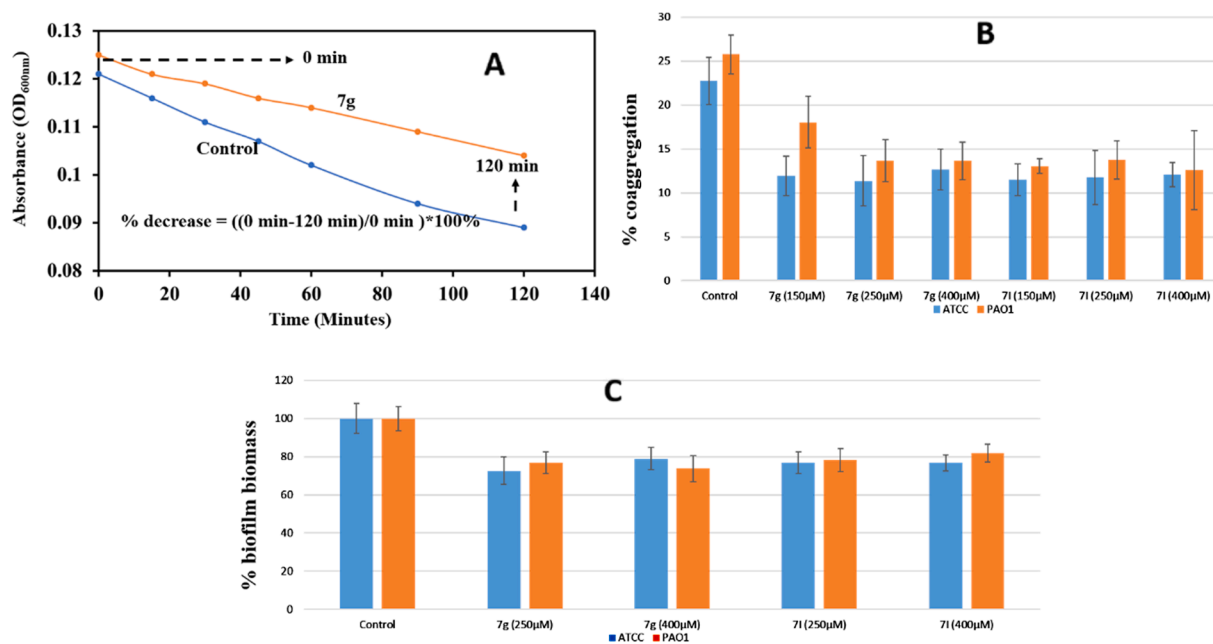


Fig. 4. Example of *P. aeruginosa* settling indicated through decrease in absorbance over time (A). Co-aggregation rate of *P. aeruginosa* PAO1 and ATCC grown in presence of 7g and 71. 7g and 71 showed significant decrease in co-aggregation percentage in comparison to the control (B). Quantification of *P. aeruginosa* biofilm biomass grown in presence of 7g and 71 (C).

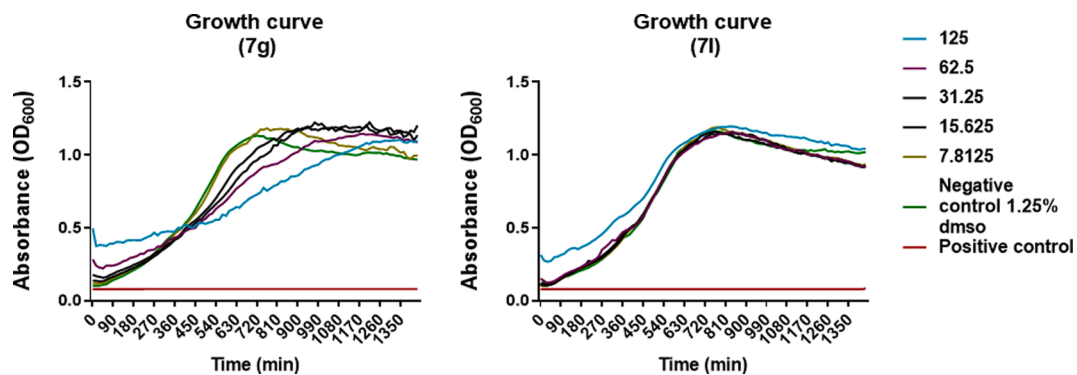


Fig. 5. Growth curve of PAO1 *P. aeruginosa*, treated with different concentrations of compound 7g or 71. Negative controls refers to DMSO (1.25%) only. Positive controls refer to blank experiment.

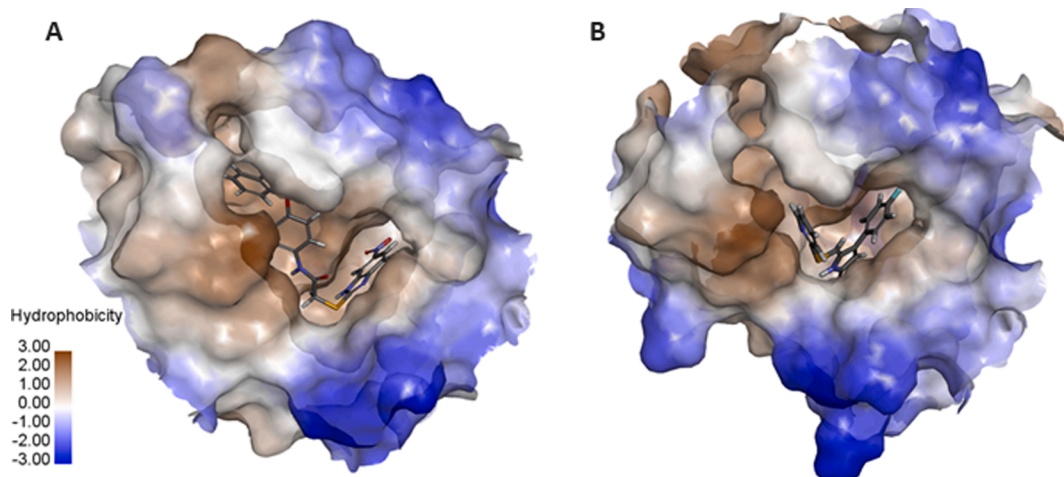


Fig. 6. Molecular docking study. Orientation (A) of ligand M-64 and (B) compound 7g in the pocket of Mvfr<sup>LBD</sup>.

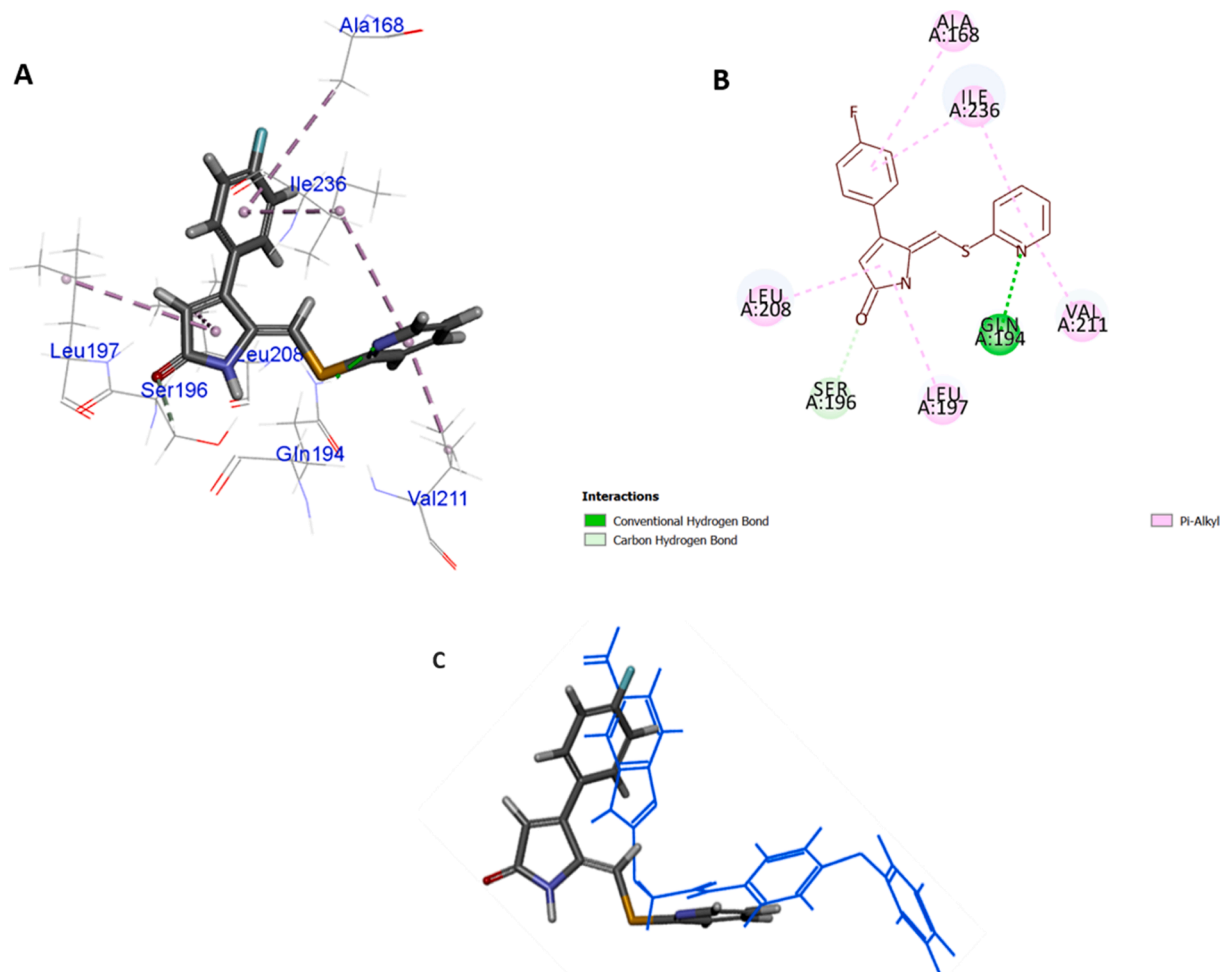


Fig. 7. (A) 3D Ligand-receptor interactions of compound 7g with Mvfr<sup>LBD</sup> (B) 2D Ligand-receptor interactions of compound 7g with Mvfr<sup>LBD</sup> (C) Overlay poses of 7g (sticks) and M-64 (blue line). (For interpretation of the references to colour in this figure legend, the reader is referred to the web version of this article.)

1632, 1324, 1124, 940, 850, 766, 732, 698; ESI-HRMS  $m/z$ : calcd for C<sub>11</sub>H<sub>8</sub>BrNO [M+Na]<sup>+</sup>: 271.9681; found 271.9683.

(Z)-5-(bromomethylene)-4-(4-fluorophenyl)-1,5-dihydro-2H-pyrrol-2-one (6b): Following the general procedure A, the title product was obtained as an off-white solid (610 mg, 76% yield); mp 128–130 °C; <sup>1</sup>H NMR (300 MHz, CDCl<sub>3</sub>) δ 7.72 (s, 1H), 7.45–7.32 (m, 2H), 7.23–7.05

(m, 2H), 6.26 (d,  $J$  = 1.8 Hz, 1H), 6.06 (s, 1H); <sup>13</sup>C NMR (101 MHz, CDCl<sub>3</sub>) δ 169.71, 165.12, 162.62, 149.39, 141.68, 130.51, 130.42, 127.19, 127.15, 122.15, 116.46, 116.25, 92.67; IR (ATR):  $\nu_{\max}$  3114, 3029, 1956, 1892, 1681, 1601, 1498, 1322, 1211, 1157, 943, 835, 700; ESI-HRMS  $m/z$ : calcd for C<sub>11</sub>H<sub>7</sub>BrFNO [M+ Na]<sup>+</sup>: 289.9587; found 289.9588.

(Z)-5-(bromomethylene)-4-(4-chlorophenyl)-1,5-dihydro-2H-pyrrol-2-one (**6c**): Following the general procedure A, the title product was obtained as an off-white solid (520 mg, 60% yield); mp 142–144 °C; <sup>1</sup>H NMR (300 MHz, CDCl<sub>3</sub>) δ 8.00 (s, 1H), 7.46–7.40 (m, 2H), 7.39–7.32 (m, 2H), 6.27 (d, *J* = 1.8 Hz, 1H), 6.06 (s, 1H); <sup>13</sup>C NMR (76 MHz, CDCl<sub>3</sub>) δ 169.60, 149.21, 141.48, 136.39, 130.29, 129.83, 129.46, 128.81, 122.40, 92.74; IR (ATR): ν<sub>max</sub> 3160, 3112, 3031, 2178, 1681, 1628, 1593, 1482, 1369, 1323, 1086, 989, 829, 700; ESI-HRMS *m/z*: calcd for C<sub>11</sub>H<sub>7</sub>BrClNO [M+Na]<sup>+</sup>: 305.9292; found 305.9293.

(Z)-5-(bromomethylene)-4-(4-bromophenyl)-1,5-dihydro-2H-pyrrol-2-one (**6d**): Following the general procedure A, the title product was obtained as an off-white solid (630 mg, 64% yield); mp 144–146 °C; <sup>1</sup>H NMR (300 MHz, CDCl<sub>3</sub>) δ 8.14 (s, 1H), 7.69–7.50 (m, 2H), 7.41–7.12 (m, 2H), 6.29 (s, 1H), 6.07 (s, 1H); <sup>13</sup>C NMR (76 MHz, CDCl<sub>3</sub>) δ 169.68, 164.54, 161.25, 149.07, 149.03, 141.39, 133.09, 132.98, 130.94, 130.83, 124.38, 124.34, 122.73, 117.18, 116.90, 115.81, 115.51, 93.05; IR (ATR): ν<sub>max</sub> 3158, 3109, 3032, 1937, 1685, 1628, 1589, 1372, 1227, 1067, 991, 825, 700; ESI-HRMS *m/z*: calcd for C<sub>11</sub>H<sub>7</sub>Br<sub>2</sub>NO [M+H]<sup>+</sup>: 329.8947; found 329.8949.

(Z)-5-(bromomethylene)-4-(2-fluorophenyl)-1,5-dihydro-2H-pyrrol-2-one (**6e**): Following the general procedure A, the title product was obtained as a white solid (620 mg, 77% yield); mp 125–127 °C; <sup>1</sup>H NMR (400 MHz, CDCl<sub>3</sub>) δ 7.89 (s, 1H), 7.49–7.39 (m, 1H), 7.34 (dd, *J* = 7.5, 1.8 Hz, 1H), 7.17–7.25 (m, 2H), 6.37 (s, 1H), 5.99 (s, 1H); <sup>13</sup>C NMR (101 MHz, CDCl<sub>3</sub>) δ 169.52, 160.91, 160.74, 156.63, 143.64, 141.23, 131.68, 131.60, 130.69, 124.75, 124.45, 124.41, 116.64, 116.42, 92.48, 92.45; IR (ATR): ν<sub>max</sub> 3154, 3033, 2754, 2114, 1894, 1700, 1626, 1482, 1447, 945, 824, 702; ESI-HRMS *m/z*: calcd for C<sub>11</sub>H<sub>7</sub>BrFNO [M+H]<sup>+</sup>: 289.9587; found 289.9588.

(Z)-5-(bromomethylene)-4-(3-fluorophenyl)-1,5-dihydro-2H-pyrrol-2-one (**6f**): Following the general procedure B, the title product was obtained as a white solid (520 mg, 64% yield); mp 129–131 °C; <sup>1</sup>H NMR (300 MHz, CDCl<sub>3</sub>) δ 8.18 (s, 1H), 7.44 (m, *J* = 8.0, 5.7 Hz, 1H), 7.23–7.02 (m, 3H), 6.31 (d, *J* = 1.8 Hz, 1H), 6.12 (s, 1H). <sup>13</sup>C NMR (76 MHz, CDCl<sub>3</sub>) δ 169.68, 164.54, 161.25, 149.07, 149.03, 141.39, 133.09, 132.98, 130.94, 130.83, 124.38, 124.34, 122.73, 117.18, 116.90, 115.81, 115.51, 93.05; IR (ATR): ν<sub>max</sub> 3123, 3004, 2756, 2052, 1930, 1703, 1632, 1565, 1333, 1245, 958, 886, 843, 785, 701; ESI-HRMS *m/z*: calcd for C<sub>11</sub>H<sub>7</sub>BrFNO [M+Na]<sup>+</sup>: 289.9587; found 289.9588.

**General procedure (B) for synthesis of thioether compounds:** A mixture of thiol (0.24 mmol) and Et<sub>3</sub>N (0.4 mmol) in dry CH<sub>2</sub>Cl<sub>2</sub> (2 mL) was added dropwise to a solution of bromo-DHP **6** (0.2 mmol) in dry DCM (5 mL) at 0 °C. The reaction was stirred at room temperature for 2 to 24 h. Progress of the reaction was monitored by TLC. After completion of the reaction, water was added. The mixture was extracted with DCM (3 × 10 mL), and the combined organic extracts were washed with brine, dried with anhydrous Na<sub>2</sub>SO<sub>4</sub> and concentrated. The crude product was purified with basic aluminium oxide column chromatography eluting with 1–2% MeOH:CH<sub>2</sub>Cl<sub>2</sub>, and the desired compound (**7**) was isolated as a yellow solid.

(Z)-4-phenyl-5-((propylthio)methylene)-1,5-dihydro-2H-pyrrol-2-one (**7a**): Following the general procedure B, the title product was obtained as a yellow solid (22 mg, 44% yield); mp 128–132 °C; <sup>1</sup>H NMR (400 MHz, CDCl<sub>3</sub>) δ 7.71 (bs, 1H), 7.50–7.42 (m, 3H), 7.42–7.35 (m, 2H), 6.14 (dd, *J* = 1.9, 0.6 Hz, 1H), 5.98 (s, 1H), 2.94–2.59 (t, 2H), 1.76–1.64 (m, 2H), 1.01 (t, *J* = 7.3 Hz, 3H); <sup>13</sup>C NMR (101 MHz, CDCl<sub>3</sub>) δ 170.12, 149.70, 135.89, 132.10, 129.53, 128.98, 128.72, 119.51, 113.61, 37.10, 23.80, 13.17; IR (ATR): ν<sub>max</sub> 790, 833, 1073, 1129, 1335, 1619, 1677, 2959, 3143; ESI-HRMS *m/z*: calcd for C<sub>14</sub>H<sub>15</sub>NOS [M+Na]<sup>+</sup>: 268.0767; found 268.0766.

(Z)-4-phenyl-5-((phenylthio)methylene)-1,5-dihydro-2H-pyrrol-2-one (**7b**): Following the general procedure B, the title product was obtained as a yellow solid (36 mg, 60% yield); mp 171–172 °C; <sup>1</sup>H NMR (400 MHz, CDCl<sub>3</sub>) δ 7.87 (s, 1H), 7.52–7.41 (m, 5H), 7.41–7.28 (m, 5H), 6.23 (d, *J* = 1.8 Hz, 1H), 6.20 (s, 1H); <sup>13</sup>C NMR (101 MHz, CDCl<sub>3</sub>) δ 170.05, 150.31, 138.01, 133.66, 131.72, 130.02, 129.74, 129.65,

129.06, 128.72, 127.99, 120.52, 110.33; IR (ATR): ν<sub>max</sub> 766, 858, 988, 1125, 1333, 1476, 1577, 1613, 1675, 3018, 3139; ESI-HRMS *m/z*: calcd for C<sub>17</sub>H<sub>13</sub>NOS [M+Na]<sup>+</sup>: 302.0610; found 302.0609.

(Z)-5-(((4-chlorophenyl)thio)methylene)-4-phenyl-1,5-dihydro-2H-pyrrol-2-one (**7c**): Following the general procedure B, the title product was obtained as a yellow solid (38 mg, 64% yield); mp 171–173 °C; <sup>1</sup>H NMR (400 MHz, CDCl<sub>3</sub>) δ 8.06 (s, 1H), 7.48–7.37 (m, 5H), 7.31 (s, 4H), 6.24 (s, 1H), 6.08 (s, 1H); <sup>13</sup>C NMR (101 MHz, CDCl<sub>3</sub>) δ 150.32, 138.79, 134.13, 132.34, 131.62, 131.20, 129.81, 129.78, 129.09, 128.69, 122.37, 108.91; IR (ATR): ν<sub>max</sub> 790, 805, 1088, 1333, 1473, 1672, 2111, 3014, 3144; ESI-HRMS *m/z*: calcd for C<sub>17</sub>H<sub>12</sub>ClNOS [M+Na]<sup>+</sup>: 336.0220; found 336.0221.

(Z)-4-phenyl-5-((pyridin-2-ylthio)methylene)-1,5-dihydro-2H-pyrrol-2-one (**7d**): Following the general procedure B, the title product was obtained as a yellow solid (34 mg, 60% yield); mp 226–227 °C; <sup>1</sup>H NMR (400 MHz, DMSO-*d*<sub>6</sub>) δ 10.45 (s, 1H), 8.46 (ddd, *J* = 4.9, 1.9, 1.0 Hz, 1H), 7.76 (ddd, *J* = 8.1, 7.4, 1.9 Hz, 1H), 7.59–7.44 (m, 6H), 7.24 (ddd, *J* = 7.4, 4.9, 1.0 Hz, 1H), 6.99 (s, 1H), 6.33–6.18 (m, 1H); <sup>13</sup>C NMR (101 MHz, DMSO-*d*<sub>6</sub>) δ 170.03, 153.69, 149.91, 149.39, 137.68, 135.95, 131.63, 129.45, 128.93, 128.06, 122.78, 121.51, 120.06, 104.42; IR (ATR): ν<sub>max</sub> 787, 811, 1118, 1332, 1415, 1575, 1675, 2794, 3013, 3135; ESI-HRMS *m/z*: calcd for C<sub>16</sub>H<sub>12</sub>N<sub>2</sub>OS [M+Na]<sup>+</sup>: 303.0562; found 303.0563.

(Z)-4-(4-fluorophenyl)-5-((phenylthio)methylene)-1,5-dihydro-2H-pyrrol-2-one (**7e**): Following the general procedure B, the title product was obtained as a yellow solid (55 mg, 92% yield); mp 202–204 °C; <sup>1</sup>H NMR (300 MHz, CDCl<sub>3</sub>) δ 7.90 (s, 1H), 7.46–7.28 (m, 6H), 7.14 (t, *J* = 8.6 Hz, 1H), 6.20 (d, *J* = 1.8 Hz, 1H), 6.12 (s, 1H); <sup>13</sup>C NMR (76 MHz, CDCl<sub>3</sub>) δ 169.91, 163.59, 149.16, 137.90, 133.57, 130.59, 130.48, 130.09, 129.69, 128.09, 120.62, 116.39, 116.10, 110.25; IR (ATR): ν<sub>max</sub> 3148, 3066, 2938, 2764, 1680, 1607, 1330, 1222, 834, 797, 678; ESI-HRMS *m/z*: calcd for C<sub>17</sub>H<sub>12</sub>FNOS [M+H]<sup>+</sup>: 298.0696; found 298.0697.

(Z)-5-(((4-chlorophenyl)thio)methylene)-4-(4-fluorophenyl)-1,5-dihydro-2H-pyrrol-2-one (**7f**): Following the general procedure B, the title product was obtained as a yellow solid (61 mg, 92% yield); mp 225–226 °C; <sup>1</sup>H NMR (400 MHz, CDCl<sub>3</sub>) δ 7.98 (bs, 1H), 7.44–7.35 (m, 2H), 7.31 (s, 4H), 7.14 (dd, *J* = 9.5, 7.7 Hz, 2H), 6.21 (d, *J* = 1.9 Hz, 1H), 6.03 (s, 1H); <sup>13</sup>C NMR (101 MHz, CDCl<sub>3</sub>) δ 169.92, 164.98, 162.49, 149.19, 138.70, 134.28, 132.17, 131.29, 130.56, 130.48, 129.84, 127.67, 127.64, 121.02, 116.41, 116.19, 108.91, 108.89; IR (ATR): ν<sub>max</sub> 3143, 3056, 2961, 2768, 1901, 1669, 1607, 1500, 1088, 1007, 790; ESI-HRMS *m/z*: calcd for C<sub>17</sub>H<sub>11</sub>ClFNOS [M+H]<sup>+</sup>: 332.0307; found 332.0306.

(Z)-4-(4-fluorophenyl)-5-((pyridin-2-ylthio)methylene)-1,5-dihydro-2H-pyrrol-2-one (**7g**): Following the general procedure B, the title product was obtained as a yellowish solid (44 mg, 73% yield); mp 214–215 °C; <sup>1</sup>H NMR (300 MHz, DMSO-*d*<sub>6</sub>) δ 10.46 (s, 1H), 8.47 (ddd, *J* = 4.9, 1.9, 0.9 Hz, 1H), 7.82–7.69 (m, 1H), 7.64–7.55 (m, 2H), 7.48 (dt, *J* = 8.1, 1.0 Hz, 1H), 7.37 (t, *J* = 8.8 Hz, 2H), 7.24 (ddd, *J* = 7.4, 4.9, 1.0 Hz, 1H), 6.96 (s, 1H), 6.28 (d, *J* = 1.6 Hz, 1H); <sup>13</sup>C NMR (76 MHz, DMSO-*d*<sub>6</sub>) δ 169.95, 153.67, 149.94, 148.26, 137.71, 135.96, 130.93, 130.82, 128.09, 122.79, 121.55, 120.24, 116.11, 115.82, 104.47; IR (ATR): ν<sub>max</sub> 3135, 2970, 2864, 2782, 1897, 1683, 1625, 1500, 1116, 808, 767; ESI-HRMS *m/z*: calcd for C<sub>16</sub>H<sub>11</sub>FN<sub>2</sub>OS [M+H]<sup>+</sup>: 299.0649; found 299.0649.

(Z)-4-(4-chlorophenyl)-5-((propylthio)methylene)-1,5-dihydro-2H-pyrrol-2-one (**7h**): Following the general procedure B, the title product was obtained as a yellow solid (20 mg, 35% yield); m.p. 146–148 °C; <sup>1</sup>H NMR (300 MHz, CDCl<sub>3</sub>) δ 8.05 (s, 1H), 7.43 (d, *J* = 8.1 Hz, 2H), 7.33 (d, *J* = 8.2 Hz, 2H), 6.13 (s, 1H), 5.95 (s, 1H), 2.81 (t, *J* = 7.2 Hz, 2H), 1.69 (h, *J* = 7.3 Hz, 2H), 1.01 (t, *J* = 7.3 Hz, 3H). <sup>13</sup>C NMR (76 MHz, CDCl<sub>3</sub>) δ 172.61, 148.36, 135.76, 135.50, 130.49, 129.99, 129.28, 119.74, 114.24, 37.17, 23.82, 13.18; IR (ATR): ν<sub>max</sub> 3571, 3138, 2958, 2922, 1954, 1676, 1616, 1332, 1090, 864, 826, 661; ESI-HRMS *m/z*: calcd for C<sub>14</sub>H<sub>14</sub>ClNOS [M+Na]<sup>+</sup>: 302.0377; found 302.0377.

(Z)-4-(4-chlorophenyl)-5-((phenylthio)methylene)-1,5-dihydro-2H-

*pyrrol-2-one (7i)*: Following the general procedure B, the title product was obtained as a yellow solid (50 mg, 80% yield); mp 209–210 °C; <sup>1</sup>H NMR (400 MHz, DMSO-*d*<sub>6</sub>) δ 10.73 – 10.16 (m, 1H), 7.56 – 7.51 (m, 4H), 7.47 – 7.27 (m, 5H), 6.31 (d, *J* = 1.6 Hz, 1H), 6.08 (s, 1H); <sup>13</sup>C NMR (101 MHz, DMSO-*d*<sub>6</sub>) δ 169.79, 147.88, 136.81, 134.19, 133.91, 130.43, 130.40, 130.29, 129.68, 128.96, 128.94, 128.91, 127.50, 120.64, 108.82; IR (ATR): ν<sub>max</sub> 3140, 3053, 3013, 2112, 1899, 1672, 1598, 1478, 1329, 1091, 826, 788; ESI-HRMS *m/z*: calcd for C<sub>17</sub>H<sub>12</sub>ClNOS [M+H]<sup>+</sup>: 314.0401; found 314.0401.

*(Z)-4-(4-chlorophenyl)-5-(((4-chlorophenyl)thio)methylene)-1,5-dihydro-2H-pyrrol-2-one (7j)*: Following the general procedure B, the title product was obtained as a yellow solid (35 mg, 50% yield); mp 243–246 °C; <sup>1</sup>H NMR (300 MHz, DMSO-*d*<sub>6</sub>) δ 10.49 (s, 1H), 7.53 (s, 4H), 7.45 (d, *J* = 2.2 Hz, 4H), 6.33 (s, 1H), 6.07 (s, 1H); <sup>13</sup>C NMR (76 MHz, DMSO-*d*<sub>6</sub>) δ 169.82, 147.95, 137.54, 134.23, 133.07, 132.16, 130.63, 130.44, 130.20, 129.53, 128.95, 120.93, 107.75; IR (ATR): ν<sub>max</sub> 3150, 3019, 2296, 1901, 1678, 1612, 1475, 1330, 1100, 1007, 795, 739; ESI-HRMS *m/z*: calcd for C<sub>17</sub>H<sub>11</sub>Cl<sub>2</sub>NOS [M+Na]<sup>+</sup>: 369.9831; found 369.9831.

*(Z)-4-(4-chlorophenyl)-5-((pyridin-2-ylthio)methylene)-1,5-dihydro-2H-pyrrol-2-one (7k)*: Following the general procedure B, the title product was obtained as a yellow solid (40 mg, 63% yield); mp 209–210 °C; <sup>1</sup>H NMR (300 MHz, DMSO-*d*<sub>6</sub>) δ 10.55 – 10.40 (s, 1H), 8.49 (ddd, *J* = 4.9, 1.8, 0.9 Hz, 1H), 7.77 (td, *J* = 7.7, 1.9 Hz, 1H), 7.64 – 7.54 (m, 4H), 7.49 (dt, *J* = 8.0, 1.0 Hz, 1H), 7.25 (ddd, *J* = 7.4, 4.8, 1.0 Hz, 1H), 6.98 (s, 1H), 6.32 (d, *J* = 1.6 Hz, 1H); <sup>13</sup>C NMR (76 MHz, DMSO-*d*<sub>6</sub>) δ 169.88, 153.62, 149.97, 148.03, 137.74, 135.70, 134.31, 130.46, 129.02, 122.81, 121.58, 120.54, 104.63; IR (ATR): ν<sub>max</sub> 3132, 2996, 2780, 1686, 1574, 1452, 1120, 1090, 862, 805; ESI-HRMS *m/z*: calcd for C<sub>16</sub>H<sub>11</sub>ClN<sub>2</sub>OS [M+H]<sup>+</sup>: 315.0353; found 315.0354.

*(Z)-4-(4-bromophenyl)-5-((propylthio)methylene)-1,5-dihydro-2H-pyrrol-2-one (7l)*: Following the general procedure B, the title product was obtained as a yellow solid (24 mg, 37% yield); mp 141–144 °C; <sup>1</sup>H NMR (400 MHz, CDCl<sub>3</sub>) δ 7.65 (bs, 1H), 7.64 – 7.54 (m, 2H), 7.31 – 7.22 (m, 2H), 6.13 (dd, *J* = 1.9, 0.6 Hz, 1H), 5.93 (s, 1H), 2.85 – 2.77 (t, 2H), 1.76 – 1.62 (m, 2H), 1.01 (t, *J* = 7.3 Hz, 3H); <sup>13</sup>C NMR (101 MHz, CDCl<sub>3</sub>) δ 169.76, 148.43, 135.48, 132.25, 130.90, 130.21, 124.01, 119.69, 37.15, 23.81, 13.16; IR (ATR): ν<sub>max</sub> 3133, 3014, 2957, 2922, 1670, 1612, 1480, 1009, 820; ESI-HRMS *m/z*: calcd for C<sub>14</sub>H<sub>14</sub>BrNOS [M+H]<sup>+</sup>: 324.0052; found 324.0053.

*(Z)-4-(4-bromophenyl)-5-((phenylthio)methylene)-1,5-dihydro-2H-pyrrol-2-one (7m)*: Following the general procedure B, the title product was obtained as a yellow solid (56 mg, 78% yield); mp 202–204 °C; <sup>1</sup>H NMR (400 MHz, CDCl<sub>3</sub>) δ 7.96 (bs, 1H), 7.63 – 7.53 (m, 2H), 7.41 – 7.27 (m, 7H), 6.22 (s, 1H), 6.12 (s, 1H); <sup>13</sup>C NMR (101 MHz, CDCl<sub>3</sub>) δ 13C NMR (76 MHz, DMSO) δ 169.78, 147.93, 136.73, 133.89, 131.86, 130.65, 129.68, 128.96, 127.49, 122.89, 120.61, 108.84; IR (ATR): ν<sub>max</sub> 3140, 3056, 3013, 2923, 2111, 1897, 1672, 1611, 1072, 823, 788; ESI-HRMS *m/z*: calcd for C<sub>17</sub>H<sub>12</sub>BrNOS [M+H]<sup>+</sup>: 357.9896; found 357.9897.

*(Z)-4-(4-bromophenyl)-5-(((4-chlorophenyl)thio)methylene)-1,5-dihydro-2H-pyrrol-2-one (7n)*: Following the general procedure B, the title product was obtained as a yellow solid (55 mg, 70% yield); mp 240–241 °C; <sup>1</sup>H NMR (300 MHz, CDCl<sub>3</sub>) δ 7.81 (s, 1H), 7.63 – 7.49 (m, 2H), 7.32 – 7.18 (m, 6H), 6.17 (d, *J* = 1.7 Hz, 1H), 5.97 (s, 1H); <sup>13</sup>C NMR (76 MHz, CDCl<sub>3</sub>) δ 170.34, 159.74, 149.05, 138.27, 135.48, 135.27, 132.38, 132.01, 131.34, 130.43, 130.17, 129.87, 124.33, 121.20, 109.07; IR (ATR): ν<sub>max</sub> 3138, 3060, 3017, 2299, 1678, 1612, 1475, 1091, 1009, 805, 738; ESI-HRMS *m/z*: calcd for C<sub>17</sub>H<sub>11</sub>BrClNOS [M+H]<sup>+</sup>: 391.9506; found 391.9506.

*(Z)-4-(4-bromophenyl)-5-((pyridin-2-ylthio)methylene)-1,5-dihydro-2H-pyrrol-2-one (7o)*: Following the general procedure B, the title product was obtained as a yellow solid (48 mg, 67% yield); mp 235–236 °C; <sup>1</sup>H NMR (300 MHz, DMSO-*d*<sub>6</sub>) δ 10.50 (s, 1H), 8.49 (ddd, *J* = 4.9, 1.9, 0.9 Hz, 1H), 7.84 – 7.65 (m, 3H), 7.61 – 7.44 (m, 3H), 7.25 (ddd, *J* = 7.4, 4.9, 1.0 Hz, 1H), 6.97 (s, 1H), 6.32 (d, *J* = 1.6 Hz, 1H); <sup>13</sup>C NMR (101 MHz, DMSO-*d*<sub>6</sub>) δ 169.86, 153.60, 149.96, 148.07, 137.72,

135.61, 131.93, 130.81, 130.69, 123.00, 122.80, 121.56, 120.51, 104.61; IR (ATR): ν<sub>max</sub> 3748, 3617, 3121, 2993, 1688, 1573, 1453, 1121, 807, 748; ESI-HRMS *m/z*: calcd for C<sub>16</sub>H<sub>11</sub>BrN<sub>2</sub>OS [M+H]<sup>+</sup>: 358.9648; found 358.9649.

*(Z)-4-(2-fluorophenyl)-5-((propylthio)methylene)-1,5-dihydro-2H-pyrrol-2-one (7p)*: Following the general procedure B, the title product was obtained as a yellow solid (27 mg, 51% yield); mp 175–176 °C; <sup>1</sup>H NMR (400 MHz, CDCl<sub>3</sub>) δ 7.83 (s, 1H), 7.42 (m, *J* = 8.2, 7.2, 5.1, 1.9 Hz, 1H), 7.32 (td, *J* = 7.4, 1.9 Hz, 1H), 7.27 – 7.09 (m, 3H), 6.22 (s, 1H), 5.89 – 5.84 (m, 1H), 2.79 (t, *J* = 7.2 Hz, 2H), 1.68 (q, *J* = 7.3 Hz, 2H), 1.00 (t, *J* = 7.3 Hz, 3H); <sup>13</sup>C NMR (101 MHz, CDCl<sub>3</sub>) δ 170.05, 161.05, 158.56, 143.02, 135.62, 131.24, 131.16, 131.11, 131.09, 124.43, 124.39, 122.13, 119.82, 119.68, 116.64, 116.42, 113.57, 37.11, 23.78, 13.14; IR (ATR): ν<sub>max</sub> 3752, 3132, 2961, 2924, 2861, 1651, 1488, 1333, 1221, 818, 790; ESI-HRMS *m/z*: calcd for C<sub>14</sub>H<sub>14</sub>FNOS [M+H]<sup>+</sup>: 264.0853; found 264.0854.

*(Z)-4-(2-fluorophenyl)-5-((phenylthio)methylene)-1,5-dihydro-2H-pyrrol-2-one (7q)*: Following the general procedure B, the title product was obtained as a yellow solid (52 mg, 87% yield); mp 170–171 °C; <sup>1</sup>H NMR (400 MHz, CDCl<sub>3</sub>) δ 7.80 (s, 1H), 7.53 – 7.29 (m, 7H), 7.26 – 7.10 (m, 3H), 6.30 (s, 1H), 6.05 (d, *J* = 1.3 Hz, 1H); <sup>13</sup>C NMR (101 MHz, CDCl<sub>3</sub>) δ 169.87, 160.26, 158.37, 143.75, 137.91, 133.73, 131.47, 131.39, 131.08, 131.05, 129.91, 129.64, 129.21, 127.93, 124.56, 124.52, 123.28, 116.69, 116.48, 109.77; IR (ATR): ν<sub>max</sub> 3126, 3061, 3018, 2762, 1909, 1677, 1476, 1327, 1102, 851, 826, 766, 736; ESI-HRMS *m/z*: calcd for C<sub>17</sub>H<sub>12</sub>FNOS [M+H]<sup>+</sup>: 298.0696; found 298.0696.

*(Z)-5-(((4-chlorophenyl)thio)methylene)-4-(2-fluorophenyl)-1,5-dihydro-2H-pyrrol-2-one (7r)*: Following the general procedure B, the title product was obtained as a yellow solid (50 mg, 75% yield); mp 208–210 °C; <sup>1</sup>H NMR (400 MHz, CDCl<sub>3</sub>) δ 7.82 (s, 1H), 7.42 (m, *J* = 8.3, 7.1, 5.2, 1.8 Hz, 1H), 7.37 – 7.28 (m, 5H), 7.24 – 7.15 (m, 2H), 6.31 (s, 1H), 5.96 (d, *J* = 1.4 Hz, 1H); <sup>13</sup>C NMR (101 MHz, CDCl<sub>3</sub>) δ 172.66, 160.50, 158.48, 143.88, 138.69, 134.09, 132.33, 131.59, 131.51, 131.05, 129.79, 124.62, 124.59, 121.80, 116.73, 116.51, 108.43; IR (ATR): ν<sub>max</sub> 3145, 3016, 2922, 1906, 1674, 1617, 1474, 1090, 816, 765; ESI-HRMS *m/z*: calcd for C<sub>17</sub>H<sub>11</sub>ClFNOS [M+H]<sup>+</sup>: 332.0307; found 332.0307.

*(Z)-4-(2-fluorophenyl)-5-((pyridin-2-ylthio)methylene)-1,5-dihydro-2H-pyrrol-2-one (7s)*: Following the general procedure B, the title product was obtained as a yellow solid (42 mg, 70% yield); mp 218–219 °C; <sup>1</sup>H NMR (400 MHz, DMSO-*d*<sub>6</sub>) δ 10.58 (s, 1H), 8.44 (ddd, *J* = 4.9, 1.9, 1.0 Hz, 1H), 7.75 (ddd, *J* = 8.0, 7.3, 1.8 Hz, 1H), 7.61 – 7.32 (m, 5H), 7.23 (ddd, *J* = 7.4, 4.9, 1.1 Hz, 1H), 6.83 (s, 1H), 6.31 (s, 1H); <sup>13</sup>C NMR (101 MHz, DMSO-*d*<sub>6</sub>) δ 169.93, 160.28, 157.82, 153.46, 149.90, 142.92, 137.70, 135.86, 131.63, 131.55, 131.33, 131.30, 124.82, 124.79, 122.75, 122.58, 121.57, 119.21, 119.07, 116.36, 116.14, 104.29; IR (ATR): ν<sub>max</sub> 3127, 2993, 2783, 2320, 1907, 1686, 1624, 1575, 1416, 1121, 825, 770; ESI-HRMS *m/z*: calcd for C<sub>16</sub>H<sub>11</sub>FN<sub>2</sub>OS [M+Na]<sup>+</sup>: 321.0468; found 321.0468.

*(Z)-4-(3-fluorophenyl)-5-((pyridin-2-ylthio)methylene)-1,5-dihydro-2H-pyrrol-2-one (7t)*: Following the general procedure B, the title product was obtained as a yellow solid (50 mg, 84% yield); mp 215–217 °C; <sup>1</sup>H NMR (300 MHz, DMSO-*d*<sub>6</sub>) δ 10.53 (s, 1H), 8.48 (ddd, *J* = 4.9, 1.9, 0.9 Hz, 1H), 7.77 (ddd, *J* = 8.1, 7.4, 1.9 Hz, 1H), 7.59 (td, *J* = 8.0, 6.0 Hz, 1H), 7.50 (dt, *J* = 8.1, 1.0 Hz, 1H), 7.44 – 7.32 (m, 3H), 7.25 (ddd, *J* = 7.4, 4.9, 1.1 Hz, 1H), 7.02 (s, 1H), 6.43 – 6.14 (m, 1H); <sup>13</sup>C NMR (76 MHz, DMSO-*d*<sub>6</sub>) δ 169.81, 163.85, 160.79, 153.61, 149.93, 147.87, 137.72, 135.57, 133.89, 131.07, 130.96, 124.86, 122.83, 121.58, 120.90, 116.42, 116.14, 115.69, 115.39, 104.72; IR (ATR): ν<sub>max</sub> 3139, 3006, 2787, 2343, 1913, 1688, 1574, 1451, 1119, 957, 842, 778; ESI-HRMS *m/z*: calcd for C<sub>16</sub>H<sub>11</sub>FN<sub>2</sub>OS [M+Na]<sup>+</sup>: 321.0468; found 321.0468.

## 5.2. GFP reporter (*pqs:gfp*) strain assay

The assay for PqsR inhibition activity was performed using the PAO1

*P. aeruginosa* strain carrying the PqsR-regulated *pqsA* promoter fused to *gfp*.<sup>38</sup> The compounds were dissolved in 100% DMSO to make 40 mM stock solutions. The test compounds (serially diluted with medium) were then incubated with overnight cultures of PAO1-*pasA-gfp* using MHB (Mueller Hinton Broth) in 96-well plates at 37 °C with intermittent shaking. Readings were taken at 15 min intervals for at least 6–8 h and both GFP fluorescence and OD<sub>600</sub> were recorded. The fluorescence values shown in the graph were normalized with respect to OD<sub>600</sub>. Negative control refers to medium containing DMSO (1.25%) as the highest concentration of the test compound. The *pqs* inhibition assay was carried out in triplicate manner.

### 5.3. Co-aggregation of *P. aeruginosa* strains

Planktonic cultures of *P. aeruginosa* ATCC 25619 and PAO1 were grown in tryptone soya broth (TSB, Oxoid, Thermo Scientific, Australia) overnight at 37 °C and 150 rpm. The cultures were then re-suspended in 5 mL TSB media at a bacterial density of OD<sub>600nm</sub> = 0.1 ± 0.02 in presence of compounds **7g** and **7l** (150, 250 and 400 µM) and DMSO (control) for 24 h, at 37 °C and 150 rpm. After 24 h growth, bacterial pellet was collected via centrifugation (5000g, 10 min, 25 °C), the supernatant was removed and the pellet were washed twice with PBS with centrifugation (5000g, 5 min, 25 °C). The pellet was finally resuspended in PBS at a density of 0.1 ± 0.02 (OD<sub>600nm</sub>) and 1 mL of the bacterial suspension was transferred into a 1 mL plastic cuvette (SARSTEDT) and its absorbance at OD<sub>600nm</sub> was measured every 15 min for up to 120 min at room temperature without agitation. The decrease in absorbance, as a result of coaggregation of bacteria and settling down due to gravity, was determined as a percentage reduction in OD after 120 min.<sup>39</sup>

$$\frac{OD_{0min} - OD_{120min}}{OD_{0min}} \times 100\% \quad (1)$$

where OD<sub>0min</sub> is the initial OD at the beginning of an experiment and OD<sub>120min</sub> is the OD after 120 min. 1 mL of PBS without bacteria was used as the blank.

### 5.4. Imaging of *P. aeruginosa* biofilms

Planktonic cultures of *P. aeruginosa* ATCC 25619 and PAO1 were grown as described above. The cultures were then resuspended in TSB media at a bacterial density of OD<sub>600nm</sub> = 0.1 ± 0.02. 1 mL of the resuspended bacterial cells were then added into 12-well plates (Corning Corp. USA) and incubated for at 37 °C and 100 rpm to initiate bacterial adhesion and biofilm growth. Where indicated, biofilm growth was also initiated in the presence of compounds **7g** and **7l** at 250 µM. As a control, *P. aeruginosa* was also grown in presence of DMSO. After 24 h, the biofilms were washed twice with PBS to remove any loosely adhered bacteria and imaged using phase contrast microscopy (Zeiss, Axio, Germany) to assess biofilm morphology as described previously.<sup>40</sup>

### 5.5. Quantification of *P. aeruginosa* biofilm biomass using crystal violet assay

*P. aeruginosa* ATCC 25619 and PAO1 planktonic cultures were grown as described above. Biofilm formation was initiated by adding 200 µL (0.1 ± 0.02 at OD<sub>600nm</sub>) of bacterial culture into 96-well plates (Corning Corp. USA) in the presence of compound **7g** and **7l** (250 and 400 µM), following by incubation at 37 °C and 100 rpm. As a control, biofilm growth was initiated in presence of DMSO. After 48 h, the wells were washed once with PBS and the attached biofilms were stained by incubation with 200 µL 0.1% (w/v) crystal violet (CV) at 37 °C, 150 rpm. After incubation for 1 h, the wells were washed three times with PBS to remove excess CV followed by drying for 15 mins at 37 °C. Then, biofilms were dissolved using 80% v/v ethanol and transferred into a new 96-well plate for biomass quantification at OD<sub>550nm</sub> using a Tecan plate

reader (Infinite M1000 pro). DMSO-treated biofilm was used as a control and normalized to 100% growth, while the percentage decrease in biofilm biomass grown in presence of compounds **7g** and **7l** was analysed with respect to the DMSO control.

### 5.6. Planktonic growth assay

An overnight culture of *P. aeruginosa* PAO1 at a concentration of 5 × 10<sup>5</sup> CFU/mL in MHB was transferred to a 96-well plate. The test compounds at a concentration of 10 mg/mL in DMSO were added to each well at a maximum concentration of 125 µg/mL and incubated for 24 h at 37 °C with intermittent agitation. The OD<sub>600</sub> was recorded for each well at 15 min intervals to measure bacterial growth. The experiment was carried out once for each compound with three technical replicates per experiment.

### 5.7. Pan assay interference compounds (PAINS) screening

PAINS are the compounds which gives false and misleading results in the biological assays mainly false positive. To determine whether our new compounds belong to these categories or not we have screened these analogues in a PAIN filter (SwissADME) and the predicted results shows that these analogues validate most of the characteristics of drug likeness and cannot be categorised as PAINS.<sup>41</sup>

### Funding

This work was supported by a Discovery Project from Australian Research Council grant (DP180100845).

### Declaration of Competing Interest

The authors declare that they have no known competing financial interests or personal relationships that could have appeared to influence the work reported in this paper.

### Acknowledgements

We thank the NMR, X-ray and BMSF facility, at Mark Wainwright Analytical Centre (MWAC), UNSW Sydney. S.Sabir would like to acknowledge UNSW TFS scholarship.

### Appendix A. Supplementary material

Supplementary data to this article can be found online at <https://doi.org/10.1016/j.bmc.2020.115967>.

### References

- 1 Driscoll JA, Brody SL, Kollef MH. The Epidemiology, Pathogenesis and Treatment of *Pseudomonas aeruginosa* Infections. *Drugs*. 2007;67(3):351–368.
- 2 Azam MW, Khan AU. Updates on the pathogenicity status of *Pseudomonas aeruginosa*. *Drug Discov Today*. 2019;24(1):350–359.
- 3 Hwang W, Yoon SS. Virulence characteristics and an action mode of antibiotic resistance in multidrug-resistant *Pseudomonas aeruginosa*. *Sci Rep*. 2019;9(1):487, 1–15.
- 4 Shrivastava SR, Shrivastava PS, Ramasamy J. World health organization releases global priority list of antibiotic-resistant bacteria to guide research, discovery, and development of new antibiotics. *J Med Soc*. 2018;32(1):76–77.
- 5 Strateva T, Mitov I. Contribution of an arsenal of virulence factors to pathogenesis of *Pseudomonas aeruginosa* infections. *Ann Microbiol*. 2011;61(4):717–732.
- 6 Harmsen M, Yang L, Pamp SJ, Tolker-Nielsen T. An update on *Pseudomonas aeruginosa* biofilm formation, tolerance, and dispersal. *FEMS Immunol Med Microbiol*. 2010;59(3):253–268.
- 7 Sharma G, Rao S, Bansal A, Dang S, Gupta S, Gabrani R. *Pseudomonas aeruginosa* biofilm: Potential therapeutic targets. *Biologicals*. 2014;42(1):1–7.
- 8 Garland M, Loscher S, Bogyo M. Chemical strategies to target bacterial virulence. *Chem Rev*. 2017;117(5):4422–4461.
- 9 Hossain MA, Sattenapally N, Parikh HI, Li W, Rumbaugh KP, German NA. Design, synthesis, and evaluation of compounds capable of reducing *Pseudomonas aeruginosa* virulence. *Eur J Med Chem*. 2020;185(111800):1–10.

- 10 Lin J, Cheng J. Quorum sensing in *Pseudomonas aeruginosa* and its relationship to biofilm development. In: *Introduction to Biofilm Engineering*. vol. 1323. American Chemical Society; 2019:1–16.
- 11 Smith RS, Iglewski BHP. *aeruginosa* quorum-sensing systems and virulence. *Curr Opin Microbiol*. 2003;6(1):56–60.
- 12 Parsek MR, Peter Greenberg E. [3] Quorum sensing signals in development of *Pseudomonas aeruginosa* biofilms. In: *Methods in Enzymology*. vol. 310. Academic Press; 1999:43–55.
- 13 Lee J, Zhang L. The hierarchy quorum sensing network in *Pseudomonas aeruginosa*. *Protein & cell*. 2015;6(1):26–41.
- 14 Pesci EC, Pearson JP, Seed PC, Iglewski BH. Regulation of las and rhl quorum sensing in *Pseudomonas aeruginosa*. *J Bacteriol*. 1997;179(10):3127–3132.
- 15 McKnight SL, Iglewski BH, Pesci EC. The *Pseudomonas* quinolone signal regulates quorum sensing in *Pseudomonas aeruginosa*. *J Bacteriol*. 2000;182(10):2702–2708.
- 16 Wade DS, Calfee MW, Rocha ER, et al. Regulation of *Pseudomonas* quinolone signal synthesis in *Pseudomonas aeruginosa*. *J Bacteriol*. 2005;187(13):4372–4380.
- 17 Soheili V, Tajani AS, Ghodsi R, Bazzaz BSF. Anti-PqsR compounds as next-generation antibacterial agents against *Pseudomonas aeruginosa*: A review. *Eur J Med Chem*. 2019;172:26–35.
- 18 Lu C, Kirsch B, Zimmer C, et al. Discovery of antagonists of PqsR, a Key Player in 2-Alkyl-4-quinolone-dependent quorum sensing in *Pseudomonas aeruginosa*. *Chem Biol*. 2012;19(3):381–390.
- 19 Soukariéh F, Williams P, Stocks MJ, Cámara M. *Pseudomonas aeruginosa* quorum sensing systems as drug discovery targets: current position and future perspectives. *J Med Chem*. 2018;61(23):10385–10402.
- 20 Muimhneacháin EÓ, Reen FJ, O'Gara F, McGlacken GP. *Org Biomol Chem*. 2018;16:169–179.
- 21 Turnpenny P, Padfield A, Barton P, et al. Bioanalysis of *Pseudomonas aeruginosa* alkyl quinolone signalling molecules in infected mouse tissue using LC–MS/MS; and its application to a pharmacodynamic evaluation of MvfR inhibition. *J Pharm Biomed Anal*. 2017;139:44–53.
- 22 Ho KKK, Cole N, Chen R, Willcox MD, Rice SA, Kumar N. Immobilization of antibacterial dihydropyrrrol-2-ones on functional polymer supports to prevent bacterial infections in vivo. *Antimicrob Agents Chemother*. 2012;56(2):1138–1141.
- 23 Ho KK, Cole N, Chen R, Willcox MD, Rice SA, Kumar N. Characterisation and *in vitro* activities of surface attached dihydropyrrrol-2-ones against Gram-negative and Gram-positive bacteria. *Biofouling*. 2010;26(8):913–921.
- 24 Kumar N, Iskander G. Novel lactams. WO2007085042, 2007.
- 25 Almohaywi B, Taunk A, Wenzholz DS, et al. Design and synthesis of lactams derived from mucochloric and mucobromic acids as *Pseudomonas aeruginosa* quorum sensing inhibitors. *Molecules*. 2018;23(5):1106.
- 26 Almohaywi B, Yu TT, Iskander G, et al. Dihydropyrrrolones as bacterial quorum sensing inhibitors. *Bioorg Med Chem Lett*. 2019;29(9):1054–1059.
- 27 Parry NJPP, Williams, P. Lactams for the treatment of bacterial respiratory tract infections. WO/2018/015279, 2018.
- 28 Soukariéh F, Liu R, Romero M, et al. Hit identification of new potent PqsR antagonists as inhibitors of quorum sensing in planktonic and biofilm grown *Pseudomonas aeruginosa*. *Front Chem*. 2020;8(204).
- 29 Fong J, Yuan M, Jakobsen TH, et al. Disulfide bond-containing ajoene analogues as novel quorum sensing inhibitors of *Pseudomonas aeruginosa*. *J Med Chem*. 2017;60(1):215–227.
- 30 Kamal AAM, Petrera L, Eberhard J, Hartmann RW. Structure–functionality relationship and pharmacological profiles of *Pseudomonas aeruginosa* alkylquinolone quorum sensing modulators. *Org Biomol Chem*. 2017;15(21):4620–4630.
- 31 Starkey M, Lepine F, Maura D, et al. Identification of anti-virulence compounds that disrupt quorum-sensing regulated acute and persistent pathogenicity. *PLoS Pathog*. 2014;10(8):e1004321.
- 32 Zhu X-F, Williams Jr HJ, Ian Scott A. An improved transient method for the synthesis of N-benzoylated nucleosides. *Synth Commun*. 2003;33(7):1233–1243.
- 33 Fleitas Martínez O, Rigueiras PO, Pires ÁDS, et al. Interference with quorum-sensing signal biosynthesis as a promising therapeutic strategy against multidrug-resistant pathogens. *Front Cell Infect Microbiol*. 2019;8(444):1–17.
- 34 Allesen-Holm M, Barken KB, Yang L, et al. A characterization of DNA release in *Pseudomonas aeruginosa* cultures and biofilms. *Mol Microbiol*. 2006;59(4):1114–1128.
- 35 Das T, Kuty SK, Kumar N, Manefield M. Pyocyanin facilitates extracellular DNA binding to *Pseudomonas aeruginosa* influencing cell surface properties and aggregation. *PLoS One*. 2013;8(3):e58299.
- 36 Swartjes JJ, Das T, Sharifi S, et al. A functional DNase I coating to prevent adhesion of bacteria and the formation of biofilm. *Adv Funct Mater*. 2013;23(22):2843–2849.
- 37 Kitao T, Lepine F, Babloudi S, et al. Molecular insights into function and competitive inhibition of *Pseudomonas aeruginosa* multiple virulence factor regulator. *mBio*. 2018;9(1). e02158-02117.
- 38 Yang L, Barken KB, Skindersoe ME, Christensen AB, Givskov M, Tolker-Nielsen T. Effects of iron on DNA release and biofilm development by *Pseudomonas aeruginosa*. *Microbiology*. 2007;153(5):1318–1328.
- 39 Liu H-H, Yang Y-R, Shen X-C, Zhang Z-L, Shen P, Xie Z-X. Role of DNA in bacterial aggregation. *Curr Microbiol*. 2008;57(2):139–144.
- 40 Sabir S, Subramoni S, Das T, Black DS, Rice SA, Kumar N. Design, synthesis and biological evaluation of novel anthraniloyl-AMP mimics as PQS biosynthesis inhibitors against *Pseudomonas aeruginosa* resistance. *Molecules*. 2020;25(13):3103, 1–17.
- 41 Baell JB, Holloway GA. New substructure filters for removal of pan assay interference compounds (PAINS) from screening libraries and for their exclusion in bioassays. *J Med Chem*. 2010;53(7):2719–2740.